


# IFIT2-depleted metastatic oral squamous cell carcinoma cells induce muscle atrophy and cancer cachexia in mice

Kuo-Chu Lai<sup>1,2,3\*</sup> , Zi-Xuan Hong<sup>4</sup>, Jyh-Gang Hsieh<sup>5,6</sup>, Hui-Ju Lee<sup>7</sup>, Muh-Hwa Yang<sup>8,9</sup>, Chia-Husu Hsieh<sup>3,10,11</sup>, Cheng-Han Yang<sup>12</sup> & Yan-Ru Chen<sup>4</sup>

<sup>1</sup>Department of Physiology and Pharmacology, College of Medicine, Chang Gung University, Taoyuan City, Taiwan; <sup>2</sup>Graduate Institute of Biomedical Sciences, College of Medicine, Chang Gung University, Taoyuan City, Taiwan; <sup>3</sup>Division of Hematology and Oncology, Department of Internal Medicine, New Taipei Municipal TuCheng Hospital (Built and Operated by Chang Gung Medical Foundation), New Taipei City, Taiwan; <sup>4</sup>Masters Program in Pharmacology & Toxicology, Department of Medicine, School of Medicine, Tzu Chi University, Hualien, Taiwan; <sup>5</sup>Department of Family Medicine, Hualien Tzu Chi Hospital, Buddhist Tzu Chi Medical Foundation, Hualien, Taiwan; <sup>6</sup>Department of Medical Humanities, School of Medicine, Tzu Chi University, Hualien, Taiwan; <sup>7</sup>Department of Research and Development, Immunwork, Inc., Taipei, Taiwan; <sup>8</sup>Division of Medical Oncology, Department of Oncology, Taipei Veterans General Hospital, Taipei, Taiwan; <sup>9</sup>Institute of Clinical Medicine, National Yang Ming Chiao Tung University, Taipei, Taiwan; <sup>10</sup>Division of Hematology and Oncology, Chang Gung Memorial Hospital, Taoyuan City, Taiwan; <sup>11</sup>College of Medicine, Chang Gung University, Taoyuan City, Taiwan; <sup>12</sup>Department of Anatomic Pathology, Chang Gung Memorial Hospital, Taoyuan City, Taiwan

## Abstract

**Background** Interferon-induced protein with tetratricopeptide repeat 2 (IFIT2) is a reported metastasis suppressor in oral squamous cell carcinoma (OSCC). Metastases and cachexia may coexist. The effect of cancer metastasis on cancer cachexia is largely unknown. We aimed to address this gap in knowledge by characterizing the cachectic phenotype of an IFIT2-depleted metastatic OSCC mouse model.

**Methods** Genetically engineered and xenograft tumour models were used to explore the effect of IFIT2-depleted metastatic OSCC on cancer cachexia. Muscle and organ weight changes, tumour burden, inflammatory cytokine profiles, body composition, food intake, serum albumin and C-reactive protein (CRP) levels, and survival were assessed. The activation of the IL6/p38 pathway in atrophied muscle was measured.

**Results** IFIT2-depleted metastatic tumours caused marked body weight loss (−18.2% vs. initial body weight,  $P < 0.001$ ) and a poor survival rate ( $P < 0.01$ ). Skeletal muscles were markedly smaller in IFIT2-depleted metastatic tumour-bearing mice (quadriceps: −28.7%, gastrocnemius: −29.4%, and tibialis: −24.3%, all  $P < 0.001$ ). Tumour-derived circulating granulocyte-macrophage colony-stimulating factor (+772.2-fold,  $P < 0.05$ ), GRO $\alpha$  (+1283.7-fold,  $P < 0.05$ ), IL6 (+245.8-fold,  $P < 0.001$ ), IL8 (+616.9-fold,  $P < 0.001$ ), IL18 (+24-fold,  $P < 0.05$ ), IP10 (+18.8-fold,  $P < 0.001$ ), CCL2 (+439.2-fold,  $P < 0.001$ ), CCL22 (+9.1-fold,  $P < 0.01$ ) and tumour necrosis factor  $\alpha$  (+196.8-fold,  $P < 0.05$ ) were elevated in IFIT2-depleted metastatic tumour-bearing mice. Murine granulocyte colony-stimulating factor (+61.4-fold,  $P < 0.001$ ) and IL6 (+110.9-fold,  $P < 0.01$ ) levels were significantly increased in IFIT2-depleted metastatic tumour-bearing mice. Serum CRP level (+82.1%,  $P < 0.05$ ) was significantly increased in cachectic shIFIT2 mice. Serum albumin level (−26.7%,  $P < 0.01$ ) was significantly decreased in cachectic shIFIT2 mice. An assessment of body composition revealed decreased fat (−81%,  $P < 0.001$ ) and lean tissue (−21.7%,  $P < 0.01$ ), which was consistent with the reduced food intake (−19.3%,  $P < 0.05$ ). Muscle loss was accompanied by a smaller muscle cross-sectional area (−23.3%,  $P < 0.05$ ). Muscle atrophy of cachectic IFIT2-depleted metastatic tumour-bearing mice (i.v.-shIFIT2 group) was associated with elevated IL6 (+2.7-fold,  $P < 0.05$ ), phospho-p38 (+2.8-fold,  $P < 0.05$ ), and atrogenin-1 levels (+2.3-fold,  $P < 0.05$ ) in the skeletal muscle. Neutralization of IL6 rescued shIFIT2 conditioned medium-induced myotube atrophy (+24.6%,  $P < 0.01$ ).

**Conclusions** Our results suggest that the development of shIFIT2 metastatic OSCC lesions promotes IL6 production and is accompanied by the loss of fat and lean tissue, anorexia, and muscle atrophy. This model is appropriate for the study of OSCC cachexia, especially in linking metastasis with cachexia.

**Keywords** Oral squamous cell carcinoma; IFIT2; Metastasis; Cachexia; Muscle atrophy; IL6

Received: 6 April 2021; Revised: 6 January 2022; Accepted: 17 January 2022

\*Correspondence to: Kuo-Chu Lai, Department of Physiology and Pharmacology, College of Medicine, Chang Gung University, Taoyuan City 33302, Taiwan. Email: kuochu@mail.cgu.edu.tw

## Introduction

Cancer cachexia is a multifactorial and devastating syndrome characterized by an ongoing loss of skeletal muscle mass that cannot be fully cured by nutritional support and leads to impaired functionality, poor quality of life and shorter survival.<sup>1</sup> The frequency of cachexia in patients with advanced cancer is high (60%),<sup>2</sup> especially in those with pancreatic cancer, gastric cancer, colorectal cancer, lung cancer, upper gastrointestinal malignancies and head and neck cancer (HNC).<sup>3</sup> Perhaps due to heterogeneity, cancer cachexia can vary according to tumour type, site, mass and mouse genotype. A complete understanding of the pathophysiology of cancer cachexia has yet to be achieved.<sup>4</sup> The loss of skeletal muscle and adipose tissue is thought to be the consequence of multiple mechanisms, including alterations in energy balance, hormonal and metabolic disturbances, and a proinflammatory/procachectic environment.<sup>4</sup>

Increased levels of proinflammatory cytokines either derived from or induced by the tumour, not endogenously derived from the mouse, represent perhaps the most common point of correlation between cancer and the prevalence of cachexia.<sup>5</sup> Interleukin (IL) 6 has been associated with cancer cachexia. In addition to its proinflammatory and immunosuppressive effects in tumours, IL6 has other functions, include stimulating C-reactive protein (CRP), inducing muscle wasting and atrophy, inducing systemic autophagy in tissue wasting and promoting successful circulating tumour cell invasion and growth at a secondary site.<sup>6</sup> Many types of cancer cells secrete IL6, and increased circulating levels of IL6 in patients are associated with weight loss and reduced survival.<sup>7</sup> IL6 mediates muscle wasting through the JAK/STAT3 pathway in the colon carcinoma 26 (C26) model.<sup>8</sup> Activation of the IL6 pathway consequently promotes downstream signalling pathways, including the JAK/STAT3 and p38 pathways, in target tissues such as hepatocytes, immune cells and skeletal muscle.<sup>6</sup> These studies indicate that IL6 could be a good marker to predict the evolution of cancer cachexia and could be a promising therapeutic strategy for attenuating cachexia progression.

Interferon-induced protein with tetratricopeptide repeat 2 (IFIT2), a member of the IFIT1 family, has been reported to be an interferon-induced cytoskeleton-associated protein that plays an antiviral role.<sup>9</sup> In addition, accumulating evidence supports its important role in tumour progression. Overexpression of IFIT2 inhibits proliferation or promotes apoptosis in a variety of cancer cell lines.<sup>10</sup> Downregulation of IFIT2 expression is associated with tumour progression and poor survival of patients with different cancers, including OSCC.<sup>11–13</sup>

Our past studies further demonstrated that IFIT2 depletion resulted in epithelial-mesenchymal transition (EMT) and 5-fluorouracil resistance and enhanced in vivo angiogenesis and metastatic colonization of OSCC cells.<sup>14–16</sup> Moreover, the expression of tumour necrosis factor  $\alpha$  (TNF $\alpha$ ) was significantly upregulated in IFIT2-depleted OSCC cells.<sup>16</sup> Recent research showed that oroxylin A, the main bioactive flavonoid extracted from *Scutellaria radix*, inhibited IFIT2 depletion-induced metastasis by suppressing C–C motif chemokine ligand (CCL) 2 signalling in OSCC.<sup>17</sup> Accordingly, IFIT2 is a key mediator in OSCC progression, especially in the metastasis stage.

Metastases and cachexia may coexist.<sup>6</sup> However, few studies have utilized animal models of metastatic disease to perform cachexia research. Accordingly, we aimed to explore the effect of metastasis induced by IFIT2 depletion on cachexia. The present study demonstrates that IFIT2 depletion not only promotes cancer metastasis but also triggers cancer cachexia. The mechanisms of IFIT2 depletion-induced cancer cachexia may be associated with tumour-derived and host-derived cytokines, such as IL6.

## Material and methods

### Cell cultures

Cells stably expressing shIFIT2 and shCTRL were established using the human OSCC cell line CAL 27 (ATCC CRL-2095) and cultured as previously described.<sup>16</sup> shIFIT2 cells were derived from a metastatic tumour formed outside the lung by an shIFIT2 clone<sup>14</sup> injected into the tail vein of a BALB/c nude mouse.<sup>16</sup> shCTRL cells were isolated from xenograft tissue formed by shCTRL clones.<sup>14,16</sup> Lentiviral transduction to establish stable IFIT2-depleted clones was performed as previously described.<sup>14</sup> The characteristics of shIFIT2 and shCTRL cells have been described previously.<sup>16</sup> The mouse muscle myoblast C2C12 cell line (BCRC 60083) was obtained from the Bioresource Collection and Research Center, Taiwan, and cultured in high-glucose Dulbecco's modified Eagle's medium (DMEM; Gibco/Thermo Fisher Scientific, Waltham, MA, USA) containing 10% foetal bovine serum (FBS; Gibco/Thermo Fisher Scientific) and penicillin–streptomycin (Gibco/Thermo Fisher Scientific) at 37°C with 5% CO<sub>2</sub>.

### In vivo shIFIT2 cachexia model

Protocols involving the care and testing of animals followed the guidelines of the Institutional Animal Care and Utilization

Committee of Tzu Chi University. Sixteen-week-old male NOD/SCID mice (body weight approximately 33–35 g) were obtained from the animal centre of Tzu Chi University (Hualien, Taiwan). To address the effect of IFIT2 depletion on OSCC cachexia, mice were randomized into four groups: (1) no treatment (control), (2) shIFIT2 cells subcutaneously injected into the lower limb flank (s.c.-shIFIT2; no metastasis), (3) shCTRL cells intravenously injected into the lateral tail vein (i.v.-shCTRL; metastasis) and (4) shIFIT2 cells intravenously injected into the lateral tail vein (i.v.-shIFIT2; metastasis). Mice were subcutaneously or intravenously injected with  $5 \times 10^5$  shIFIT2 or shCTRL OSCC cells. Both control and tumour-bearing mice were assessed for changes in body weight every 3 days over the duration of the experiment. Mouse survival was monitored for 8 weeks. We found that cachectic mice died very quickly (within 2–3 days) after they lost more than 15% of their initial body weight (IBW). For experiments, such as cytokine profiling and food intake assessments, tumour-bearing mice were humanely sacrificed if they lost 15% or more of their IBW or 8 weeks after tumour cell inoculation. At the time of euthanization, skeletal muscles, organs and tumours were surgically excised, weighed, rinsed, fixed and subjected to pathological examination. Moreover, blood was collected by cardiac puncture for cytokine profiling and ELISA.

### *Histology and immunohistochemistry*

Five-micrometre paraffin-embedded tissue sections were stained with haematoxylin and eosin according to standard procedures. Immunohistochemistry was performed as described previously,<sup>14</sup> and images were analysed by a well-trained pathologist. The gastrocnemius sections were stained with a primary anti-IL6 antibody (#ARG56625; 1:200; Arigo Biolaboratories, Hsinchu, Taiwan), and the reactions were then visualized by Novolink Polymer Detection Systems (#RE7140-K, Buffalo Grove, IL, USA) according to the manufacturer's instructions.

### *Assessment of body composition and food intake*

The whole-body composition and food intake of mice at Week 7 after tumour inoculation were assessed by Minispec LF50 TD-NMR technology and Tecniplast® Metabolic Cages (24-h recording) from the Taiwan Mouse Clinic (Taipei, Taiwan).

### *Evaluation of muscle cross-sectional area*

In the assessment of gastrocnemius muscle morphology and cross-sectional area (CSA), haematoxylin and eosin staining was used to examine muscle fibres ( $n = 300$ – $400$  per muscle) using ImageJ software (NIH, Bethesda, MA, USA).<sup>18</sup>

### *Measurement of in vivo cytokine, albumin and C-reactive protein levels*

At the time of euthanization, mouse blood was collected by cardiac puncture. Aliquots of collected sera were stored at  $-80^\circ\text{C}$  until multiplexing. One hundred microliters of serum per sample was subjected to serum cytokine profiling by the National Applied Research Laboratories (NARLabs, Taipei, Taiwan). Milliplex MAP human HCYTA-60K-PX48 and mouse MCYTMA-70K-PX32 panels (Merck KGaA, Darmstadt, Germany) were used to determine the circulating levels of human and murine cytokines, respectively, in sera from cachectic mice. Serum albumin levels were detected by a Fuji Dri-chem Nx500 (Fujifilm Co., Tokyo, Japan) according to the manufacturer's instructions. Serum CRP was measured by an ELISA Kit (# ab157712, Abcam, Cambridge, MA, USA) according to the manufacturer's instructions.

### *Quantitative real-time polymerase chain reaction*

Total RNA was isolated from gastrocnemius muscle using TRIzol reagent. Quantitative real-time polymerase chain reaction was performed as described previously.<sup>16</sup> The primers used are listed in Supporting Information, Table S1.

### *Western blotting*

Western blotting was performed as described previously.<sup>17</sup> Commercially available antibodies targeting the following proteins were purchased: IL6 (#GTX110527) and GAPDH (#GTX627408) from GeneTex (Irvine, CA, USA), STAT3 (#4904) and phospho-STAT3-Y705 (#9131) from Cell Signalling, p38 (bs-0637R) from Bioss (Woburn, MA, USA), phospho-p38 MAPK (T180/Y182) (#3438-100) from BioVision (Milpitas, CA, USA), and Atrogin-1 (#ab74023) from Abcam. The bound antibody was visualized by chemiluminescence using the UVP BioSpectrum Imaging System (Analytic Jena US, Jena, Germany). Band intensities were quantified by ImageJ software (NIH) and were normalized to the GAPDH density for each target.

### *Conditioned medium collection*

ShIFIT2 cells were seeded into 10-cm dishes containing DMEM with 10% FBS. After 16–18 h of incubation, the growth medium was removed, and the cells were washed twice with PBS. Fresh medium without FBS was added for 48 h, and the medium was collected and centrifuged at 3000 rpm for 5 min. Aliquots of the medium were stored at  $-80^\circ\text{C}$ .

### Conditioned medium myotube atrophy model

The experiment was carried out as previously described<sup>19</sup> with modifications. C2C12 cells were cultured and switched to differentiation medium (DM) for 4 days. The DM for C2C12 cells was high-glucose DMEM with 2% horse serum (GE Healthcare, Chicago, Illinois, USA). After 4 days in differentiation, cells were then treated with DM (as a control), 50% shIFIT2 conditioned medium (CM) in DM with or without neutralizing IL6 Antibody (#MAB2061; R&D systems, Minneapolis, MN, USA) for 3 days. Control and experimental cells were given fresh medium every 24 h. Myotubes were washed with PBS and fixed with ice-cold 100% methanol. Fixed cells were permeabilized with 0.3% Triton X-100, blocked in 2% BSA-PBS for 1 h at room temperature and immunostained with Alexa Fluor 488-conjugated Myosin 4 Monoclonal Antibody overnight at 4°C (#53-6503-82; 1:500; Thermo Fisher Scientific). Myotubes were photographed by a DS-Qi2 camera with NIS-Elements Software (Nikon, Tokyo, Japan). Average myotube diameter per well was measured in a total of 50 myotubes from at least 5 random fields using ImageJ software (NIH). Three independent wells were used to calculate mean values for control and treated myotubes.

### Statistical analysis

Data are presented as the mean  $\pm$  standard error of the mean. SigmaPlot Version 13.0 (Systat Software, San Jose, CA) was used to create the figures. Multiple comparisons were analysed by one-way analysis of variance followed by Tukey's multiple comparison post hoc analysis. In cases where there was unequal variance or an unequal  $n$  among the three groups, a non-parametric post hoc test (Dunn's) was used. Survival analysis was performed using the Kaplan–Meier log-rank test. A  $P$  value less than 0.05 was considered to indicate significance.

## Results

### The *i.v.-shIFIT2* tumours caused significant body weight loss

To ascertain the effect of IFIT2 depletion on OSCC cachexia, mice were randomized into four treatment groups (Figure 1A). The *s.c.-shIFIT2* and *i.v.-shIFIT2* groups were compared to clarify whether cancer cachexia induced by IFIT2 depletion is associated with metastasis, whereas the *i.v.-shCTRL* and *i.v.-shIFIT2* were compared to determine whether cancer cachexia is associated with IFIT2 depletion.

After an initial lag phase, *i.v.-shIFIT2* tumour-bearing mice had significantly lower body weights than mice in the other groups, including the healthy control, *s.c.-shIFIT2* and

*i.v.-shCTRL* groups (Figure 1B). There were no significant differences in the body weight curves in the healthy control, *s.c.-shIFIT2* and *i.v.-shCTRL* groups. Consistent with the difference in the body weight curve, the final body weight and tumour-free body weight were significantly lower in the *i.v.-shIFIT2* group than in the healthy control group (Figure 1C). Compared with healthy control mice, *i.v.-shIFIT2* tumour-bearing mice showed a significant reduction in weight gain (Figure 1D). By comparison with the IBW, the weight of control mice increased by 2.85 g, the weight of *s.c.-shIFIT2* and *i.v.-shCTRL* mice slightly decreased (by 0.11 and 0.01 g, respectively), and the weight of *i.v.-shIFIT2* mice had decreased by 6.43 g at the time of euthanization. No ascites was observed in *s.c.-shIFIT2*, *i.v.-shCTRL* and *i.v.-shIFIT2* groups (Figure S1), indicating that weight change of tumour-bearing mice was not due to ascites. There were no significant differences in survival among the control, *i.v.-shCTRL* and *s.c.-shIFIT2* groups. However, the survival of the *i.v.-shIFIT2* group was significantly decreased (Figure 1E).

### *i.v.-shIFIT2* tumours cause significant muscle weight loss

To verify that body weight loss was associated with muscle and organ loss, several skeletal muscles were collected and weighed. Except for the quadriceps, none of the muscles showed a significant difference in weight between the control and *s.c.-shIFIT2* mice (Figure 2A). Similarly, there was no significant difference in muscle weight between the healthy control and *i.v.-shCTRL* mice. However, the quadriceps, gastrocnemius and tibialis anterior weights were significantly reduced in *i.v.-shIFIT2* mice compared with healthy control mice (Figure 2A). Except for those in the *s.c.-shIFIT2* group, tumour-bearing mice showed no significant difference in liver weight compared with healthy control mice (Figure 2B). No significant differences in spleen weight were observed among these four groups (Figure 2C). Histological examination revealed no metastasis or obvious pathogenic alterations in the livers and spleens of these four groups.

To assess the association of tumour burden and weight loss in the shIFIT2 cachexia model, subcutaneous tumours from *s.c.-shIFIT2* mice and metastatic tumours formed outside the lung from *i.v.-shCTRL* and *i.v.-shIFIT2* mice were collected and weighed. No metastatic tumours were found in *s.c.-shIFIT2* mice. Consistent with the results of a previous study,<sup>14</sup> *i.v.-shCTRL* tumour nodules were predominantly localized in the lungs, whereas *i.v.-shIFIT2* tumours were present in the lungs as well as the thoracic, peritoneal and retroperitoneal cavities (Table 1). The mean subcutaneous tumour weight was 1.3 g in *s.c.-shIFIT2* mice, whereas the mean metastatic tumour weights were 0.1 and 0.67 g in *i.v.-shCTRL* and *i.v.-shIFIT2* mice, respectively (Figure 2D). Furthermore, we measured the lung weight of mice in the four groups

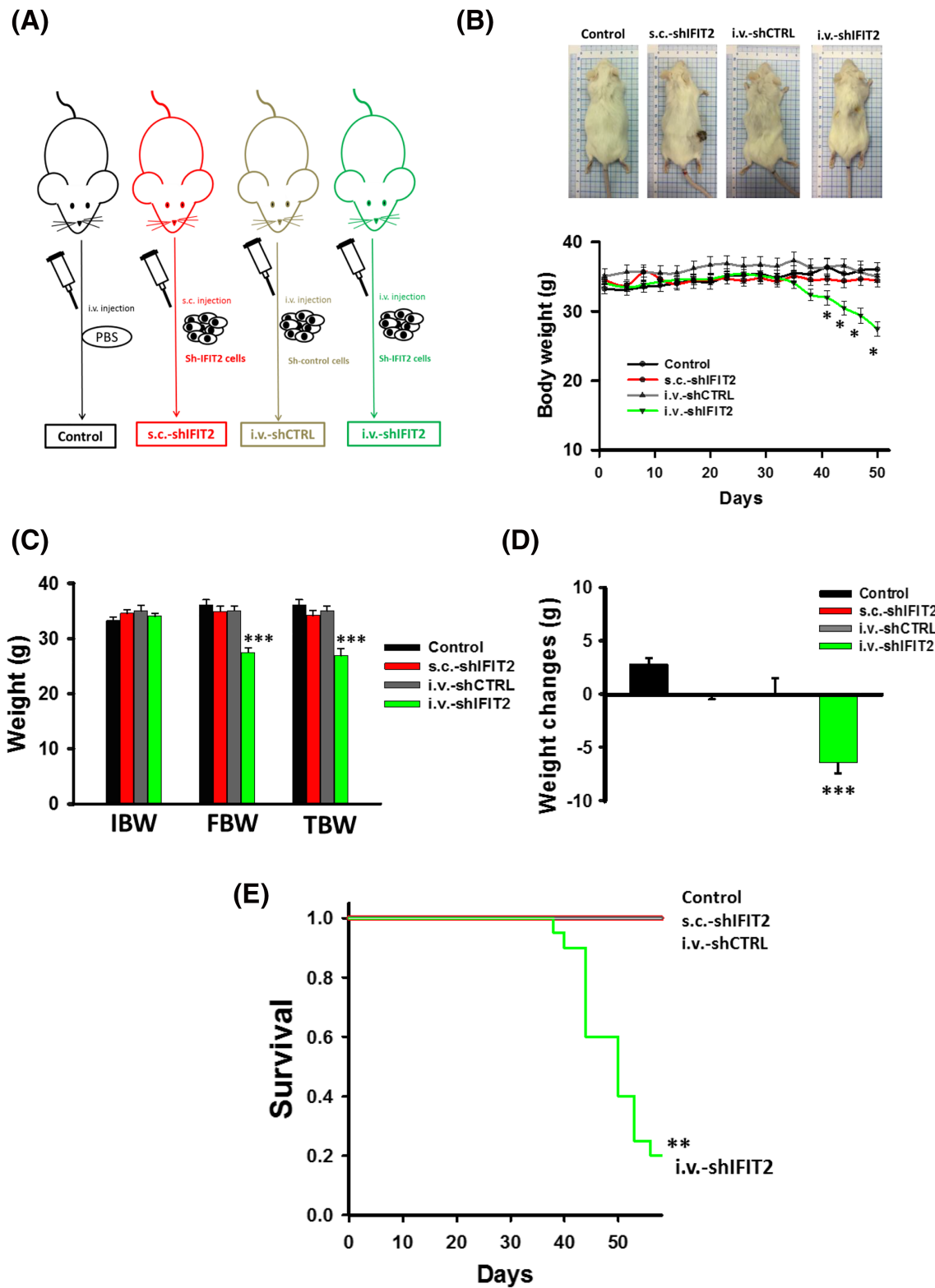


**Figure 1** The i.v.-shIFIT2 tumours caused significant body weight loss and a poor survival rate. (A) Schematic representation of the experimental design. (B) Body weight curve over the entire experimental period. (C) Initial body weight (IBW), final body weight (FBW) and final tumour-free body weight (TBW) of these four groups. (D) Body weight change and (E) survival of mice in these four groups, including the healthy control ( $n = 9$ ), s.c.-shIFIT2 ( $n = 9$ ), i.v.-shCTRL ( $n = 9$ ), and i.v.-shIFIT2 ( $n = 20$ ) groups. Data are presented as the mean  $\pm$  SEM. \* $P < 0.05$ , \*\* $P < 0.01$  and \*\*\* $P < 0.001$  compared with the control group.

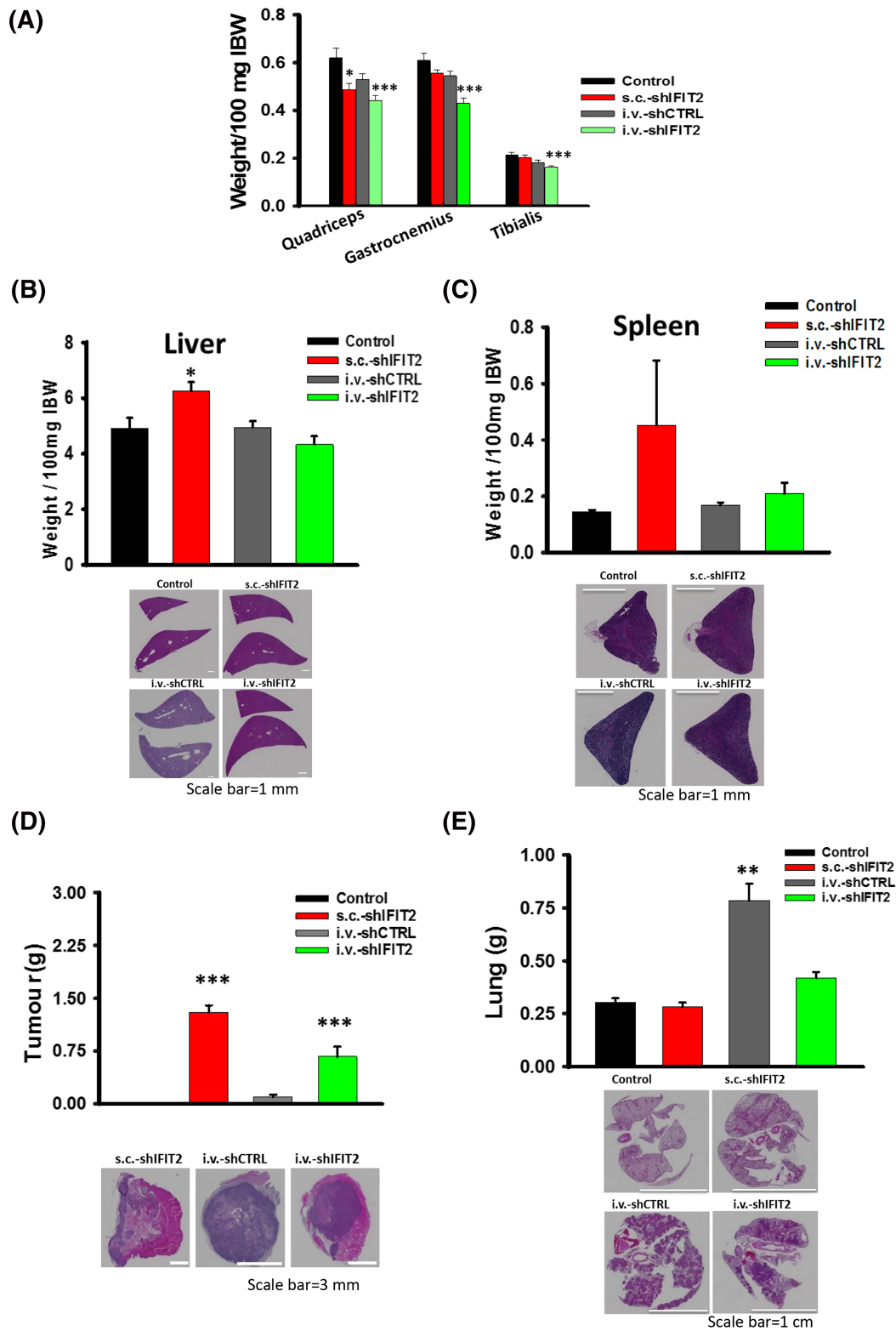


**Figure 2** The i.v.-shIFIT2 tumours caused significant muscle weight loss in mice. (A) Quadriceps, gastrocnemius and tibialis weights. (B) Liver, (C) spleen, (D) tumour and (E) lung weights and representative photomicrograph of haematoxylin and eosin-stained sections at the time of euthanization of control ( $n = 9$ ), s.c.-shIFIT2 ( $n = 9$ ), i.v.-shCTRL ( $n = 9$ ) and i.v.-shIFIT2 ( $n = 20$ ) mice. Muscle, liver and spleen weights were normalized to the IBW, and the results are reported as weight/100 mg IBW. Data are presented as the mean  $\pm$  SEM. \* $P < 0.05$ , \*\* $P < 0.01$  and \*\*\* $P < 0.001$  compared with the control group. IBW, initial body weight.



**Table 2** Human cytokine concentrations in sera of control, s.c.-shIFIT2, i.v.-shCTRL and i.v.-shIFIT2 hosts

Cytokine (pg/mL)	Control (n = 4) Mean (SEM)	s.c.-shIFIT2 (n = 6) Mean (SEM)	i.v.-shCTRL (n = 7) Mean (SEM)	i.v.-shIFIT2 (n = 7) Mean (SEM)
sCD40L	n.d. (<0.13)	37.56 (9.67)	52.95 (19.46)	40.50 (5.5)
EGF	7.50 (1.32)	6.76 (0.88)	5.59 (1.24)	4.52 (0.54)
Eotaxin	n.d. (<2.04)	4.74 (0.6)	7.24 (0.89)	9.26 (2.82)
FGF-2	227.73 (196.16)	18.06 (2.11)	161.57 (89.36)	386.34 (254.61)
FLT-3L	5.19 (0.58)	4.82 (0.29)	6.48 (0.94)	3.30 (0.46)
Fractalkine	50.71 (13.67)	56.12 (6.39)	127.03 (27.95)	83.87 (11.43)
G-CSF	n.d. (<2.52)	n.d. (<2.52)	n.d. (<2.52)	n.d. (<2.52)
GM-CSF	n.d. (<0.16)	n.d. (<0.16)	n.d. (<0.16)	123.55 (70.95)
GRO $\alpha$	n.d. (<0.11)	28.56 (9.53)	2.98 (0.45)	141.21 (92.14)
IFN $\alpha$ 2	n.d. (<2.11)	3.61 (0.71)	6.58 (1.3)	8.15 (1.67)
IFN $\gamma$	n.d. (<0.77)	n.d. (<0.77)	n.d. (<0.77)	n.d. (<0.77)
IL1 $\alpha$	n.d. (<0.2)	0.60 (0.2)	n.d. (<0.2)	11.73 (8.6)
IL1 $\beta$	n.d. (<0.87)	n.d. (<0.87)	9.44 (2.26)	n.d. (<0.87)
IL1RA	n.d. (<0.23)	0.62 (0.21)	1.99 (0.31)	2.08 (0.74)
IL2	n.d. (<0.67)	n.d. (<0.67)	n.d. (<0.67)	n.d. (<0.67)
IL3	n.d. (<2.75)	n.d. (<2.75)	n.d. (<2.75)	n.d. (<2.75)
IL4	n.d. (<0.52)	n.d. (<0.52)	n.d. (<0.52)	n.d. (<0.52)
IL5	n.d. (<0.01)	0.15 (0.06)	0.31 (0.08)	0.40 (0.07)
IL6	n.d. (<0.79)	7.97 (4.31)	1.63 (0.37)	194.19 (96.98)
IL7	n.d. (<1.3)	n.d. (<1.3)	n.d. (<1.3)	n.d. (<1.3)
IL8	n.d. (<0.72)	107.73 (32.91)	27.08 (5.42)	444.17 (193.16)
IL9	n.d. (<0.02)	n.d. (<0.02)	1.43 (0.52)	n.d. (<0.02)
IL10	n.d. (<0.29)	0.96 (0.26)	1.64 (0.37)	0.86 (0.16)
IL12 (p40)	2.41 (0.81)	2.79 (0.31)	4.17 (1.02)	77.82 (72.93)
IL12 (p70)	n.d. (<0.33)	n.d. (<0.33)	3.82 (0.92)	1.06 (0.33)
IL13	9.05 (4.33)	4.29 (1.37)	18.51 (4.72)	9.12 (2.35)
IL15	n.d. (<0.07)	0.58 (0.24)	0.98 (0.34)	4.75 (1.33)
IL17A	n.d. (<0.93)	n.d. (<0.93)	3.14 (0.76)	n.d. (<0.93)
IL17E/IL-25	9.16 (2.92)	8.95 (2.50)	10.45 (3.22)	11.59 (2.99)
IL17F	n.d. (<0.86)	n.d. (<0.86)	2.74 (0.75)	n.d. (<0.86)
IL18	n.d. (<0.67)	7.33 (0.60)	8.68 (2.14)	16.08 (7.07)
IL22	n.d. (<10.32)	n.d. (<10.32)	n.d. (<10.32)	n.d. (<10.32)
IL27	36.13 (17.01)	29.26 (12.33)	68.64 (15.87)	6.22 (1.61)
IP10	2.63 (0.51)	21.66 (3.94)	6.54 (0.69)	49.38 (15.52)
CCL2	1.57 (0.61)	249.76 (62.8)	8.37 (1.75)	689.54 (162.19)
MCP-3	2.53 (0.24)	n.d. (<1.98)	7.47 (1.81)	n.d. (<1.98)
M-CSF	n.d. (<0.58)	1.12 (0.26)	3.32 (0.83)	7.30 (4.67)
CCL22	n.d. (<0.56)	2.19 (0.7)	n.d. (<0.56)	5.11 (1.38)
MIG	n.d. (<1.27)	n.d. (<1.27)	8.51 (2.14)	4.80 (1.19)
MIP1 $\alpha$	n.d. (<8.09)	n.d. (<8.09)	n.d. (<8.09)	n.d. (<8.09)
MIP1 $\beta$	n.d. (<0.67)	1.46 (0.15)	1.95 (0.31)	1.33 (0.13)
PDGF-AA	5.49 (2.79)	9.14 (0.71)	18.41 (4.92)	6.19 (1.54)
PDGF-AB/BB	552.33 (60.8)	511.07 (23.82)	605.10 (72.61)	373.81 (55.3)
RANTES	1.71 (0.15)	1.39 (0.09)	1.36 (0.26)	1.28 (0.38)
TGF $\alpha$	n.d. (<1.31)	n.d. (<1.31)	n.d. (<1.31)	n.d. (<1.31)
TNF $\alpha$	n.d. (<0.06)	3.03 (0.48)	2.13 (0.61)	11.81 (3.96)
TNF $\beta$	n.d. (<1.4)	n.d. (<1.4)	n.d. (<1.4)	n.d. (<1.4)
VEGF $\alpha$	12.21 (5.06)	4.14 (0.94)	3.22 (0.84)	n.d. (<0.47)

n.d., not detected; SEM, standard error of the mean.

body and muscle weights, higher levels of tumour-derived and host-derived cytokines, such as IL6, and a worse survival rate than healthy control mice. Accordingly, we suggest that IFIT2-depleted metastatic tumour-induced cachexia is strongly associated with inflammation.

### *The i.v.-shIFIT2 mice exhibited a loss of body composition and decreased food intake*

To understand the effects of shIFIT2 tumours on body composition, control, s.c.-shIFIT2 and i.v.-shIFIT2 mice were

assessed. The amount of total fat was significantly reduced in i.v.-shIFIT2 mice compared with healthy control mice (Figure 4A), and the amount of lean tissue was significantly reduced in i.v.-shIFIT2 mice compared with healthy control and s.c.-shIFIT2 mice (Figure 4B). The role of anorexia and reduced food intake varies among animal models of cachexia.<sup>21</sup> Therefore, the effects of shIFIT2 tumours on food and water intake were further examined. The 24-h average dry food intake of i.v.-shIFIT2 mice was significantly reduced compared with that of healthy control mice (Figure 4C). In addition, the 24-h average water intake of i.v.-shIFIT2 mice was significantly reduced compared with that of s.c.-shIFIT2 mice



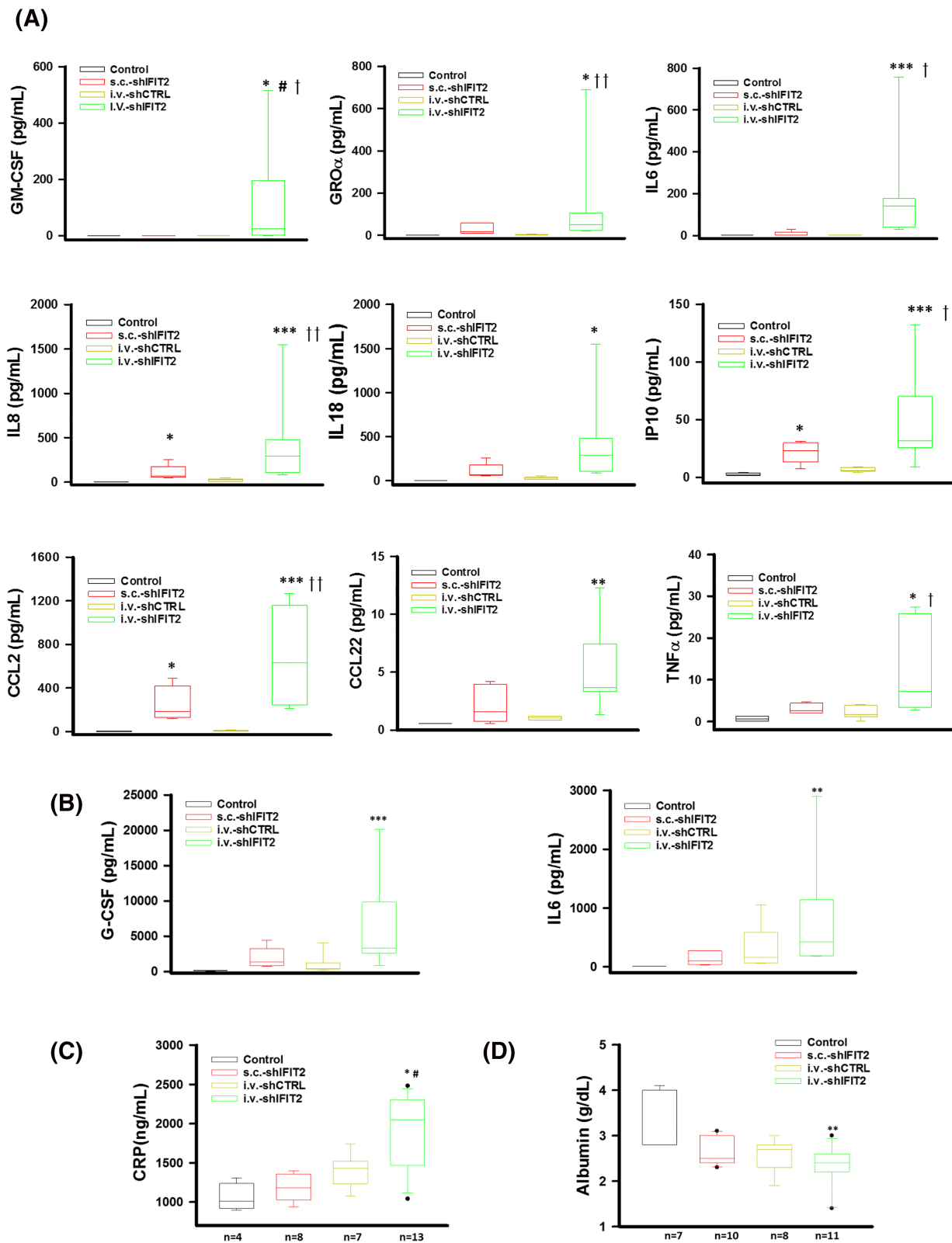


**Figure 3** Elevated inflammatory response in cachectic i.v.-shIFIT2 mice. (A) Human and (B) murine cytokine levels in sera from control ( $n = 4$ ), s.c.-shIFIT2 ( $n = 6$ ), i.v.-shCTRL ( $n = 7$ ) and i.v.-shIFIT2 mice ( $n = 7$ ). (C) Serum CRP and (D) serum albumin levels in control, s.c.-shIFIT2, i.v.-shCTRL and i.v.-shIFIT2 mice. \* $P < 0.05$ , \*\* $P < 0.01$  and \*\*\* $P < 0.001$  compared with the control group. # $P < 0.05$  compared with the s.c.-shIFIT2 group. † $P < 0.05$ , and †† $P < 0.01$  compared with the i.v.-shCTRL group.

**Table 3** Murine cytokine concentrations in sera of control, s.c.-shIFIT2, i.v.-shCTRL and i.v.-shIFIT2 hosts

Cytokine (pg/mL)	Control (n = 4) Mean (SEM)	s.c.-shIFIT2 (n = 6) Mean (SEM)	i.v.-shCTRL (n = 7) Mean (SEM)	i.v.-shIFIT2 (n = 7) Mean (SEM)
G-CSF	109.82 (17.82)	1930.21 (604.5)	1003.83 (517.89)	6743.28 (2527.3)
Eotaxin	1200.95 (102.13)	1445.83 (56.64)	1238.71 (167.78)	1308.95 (152.79)
GM-CSF	n.d. (<17.8)	52.44 (3.84)	60.70 (4.11)	17.79 (3.39)
IFN $\gamma$	n.d. (<6.18)	14.88 (1.13)	17.10 (0.76)	n.d. (<6.18)
IL1 $\alpha$	1201.13 (300.51)	272.88 (27.54)	238.08 (18.5)	911.66 (176.06)
IL1 $\beta$	4.1 (0.55)	8.60 (1.88)	9.04 (0.74)	4.76 (0.39)
IL2	n.d. (<3.6)	11.22 (2.7)	9.08 (1.77)	7.94 (2.01)
IL4	n.d. (<5.88)	14.73 (2.07)	7.5 (1.35)	n.d. (<5.88)
IL3	n.d. (<3.26)	3.07 (0.52)	2.97 (0.55)	n.d. (<3.26)
IL5	n.d. (<6.6)	12.74 (1.26)	13.49 (1.06)	n.d. (<6.6)
IL6	7.69(1.04)	135.10 (46.49)	311.87 (142.26)	852.35 (368.56)
IL7	n.d. (<5.54)	n.d. (<5.61)	n.d. (<5.61)	n.d. (<5.54)
IL9	156.74 (41.57)	508.29 (109.52)	684.27 (111.44)	254.52 (39.99)
IL10	n.d. (<6.64)	14.17 (1.94)	14.06 (0.6)	18.51 (4.1)
IL12 (p40)	7.08 (0.52)	6.98 (1.16)	8.97 (2.02)	7.89 (0.75)
IL12 (p70)	n.d. (<7.96)	67.06 (6.02)	58.36 (3.17)	14.41 (2.93)
LIF	n.d. (<5.92)	n.d. (<6.01)	70 (18.01)	13.82 (1.97)
IL13	34.30 (2.29)	176.58 (4.61)	179.70 (6.9)	50.15 (2.6)
LIX	n.d. (>20134)	4586 (420.32)	4129.57 (393.73)	17147.5 (3470.28)
IL15	n.d. (<52.92)	58.29 (5.55)	59.44 (7.06)	n.d. (<52.92)
IL17	11.35 (0.57)	9.90 (0.74)	10.60 (1.72)	12.59 (2.75)
IP10	308.35 (34.55)	527.50 (22.66)	668.76 (36.21)	308.29 (28.19)
GRO $\alpha$	194.27 (49.18)	451.31 (28.77)	426.66 (23.25)	122.27 (29.98)
CCL2	58.34 (10.39)	179.01 (24.35)	156.32 (18.16)	155.60 (27.71)
MIP1 $\alpha$	39.87 (6.38)	104.24 (4.57)	105.09 (3.66)	57.66 (5.39)
MIP1 $\beta$	63.79 (7.67)	112.03 (2.85)	122.16 (4.31)	53.40 (8.01)
M-CSF	8.85 (0.73)	29.23 (2.11)	31.15 (1.4)	10.19 (0.77)
MIP-2	273.02 (19.1)	164.0 (6.75)	197.31 (18.73)	210.51 (12.64)
MIG	95.34 (13.71)	196.69 (13.71)	160.75 (26.18)	80.82 (12.07)
RANTES	79.78 (10.13)	68.30 (3.18)	84.29 (11.12)	36.89 (4.92)
VEGF	n.d. (<4.02)	8.89 (0.44)	10.19 (1.23)	n.d. (<4.12)
TNF $\alpha$	11.73 (0.68)	15.35 (0.87)	18.00 (0.84)	15.04 (1.08)

n.d., not detected; SEM, standard error of the mean.

(Figure 4D). These results indicate that body weight loss in cachectic i.v.-shIFIT2 mice may be associated with anorexia. Moreover, we found that lean body mass may be a significant predictor of cachexia in the shIFIT2 cachexia model.

### *IL6/p38 signalling is associated with muscle atrophy in the shIFIT2 cachexia model*

To address whether the muscle weight loss of cachectic shIFIT2 mice was due to muscle atrophy, the gastrocnemius muscle fibre CSA was examined, and we found significant myofibre atrophy in i.v.-shIFIT2 mice, with a 23.3% decrease in the mean gastrocnemius muscle fibre CSA (Figure 5A). Myogenic dysregulation may promote cancer-induced muscle wasting<sup>5</sup>; thus, we assessed the expression of myogenic markers, such as MyoG, that are induced by MyoD. We observed that MyoG and MyoD expression did not significantly change in muscle from cachectic i.v.-shIFIT2 mice (Figure 5B), indicating that myogenic dysfunction may not be involved in muscle wasting in the shIFIT2 cachexia model. Simultaneously, the gastrocnemius mRNA expression levels of E3 ubiquitin ligases MuRF-1 and atrogen-1 were significantly

increased in i.v.-shIFIT2 mice compared with healthy control mice (Figure 5B), indicating that ubiquitin proteasome system is critically necessary for muscle wasting in the shIFIT2 cachexia model.

IL6 has emerged as a critical factor related to muscle wasting in cachexia mice. Thus, to link IL6 to muscle wasting, we examined IL6 expression in the fast glycolytic fibres of gastrocnemius muscles, which are sensitive to cachectic stimuli.<sup>20</sup> IL6 protein levels in the gastrocnemius muscle were increased in shIFIT2 mice, especially in i.v.-shIFIT2 mice, as determined by immunohistochemistry and western blotting (Figure 5C and D). Moreover, the protein levels of phospho-p38 and atrogen-1 in the gastrocnemius muscle were significantly increased in i.v.-shIFIT2 mice compared with healthy control and s.c.-shIFIT2 mice (Figure 5D). Consistently, we found that shIFIT2 CM-treated differentiated C2C12 myotubes had significantly smaller diameters compared with those treated with control, whereas treatment with anti-IL6 antibody (0.2  $\mu$ g/mL) rescued shIFIT2 CM-induced myotube atrophy (Figure 5E and F). These results indicate that IL6 signalling may play an important role in mediating the skeletal muscle atrophy in the shIFIT2 cachexia model.

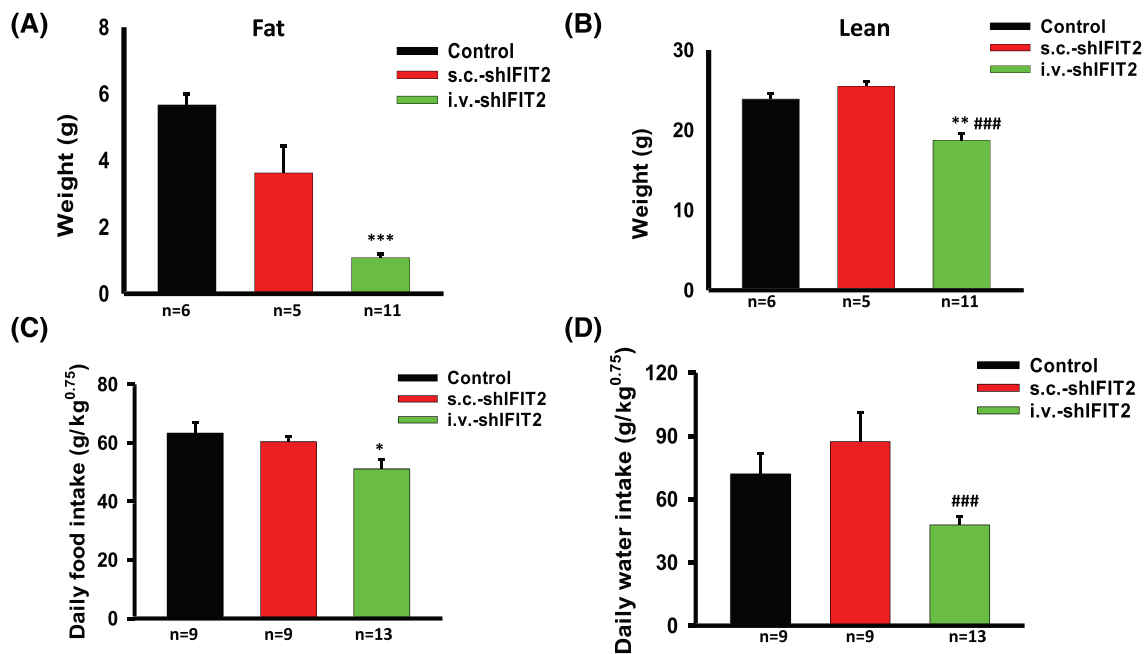


**Figure 4** The i.v.-shIFIT2 tumours caused a significant loss of body composition and anorexia in mice. (A) Fat and (B) lean weights of control, s.c.-shIFIT2 and i.v.-shIFIT2 mice. (C) Average 24-h food and (D) water intake by control, s.c.-shIFIT2 and i.v.-shIFIT2 mice. Data are presented as the mean  $\pm$  SEM. \* $P < 0.05$ , \*\* $P < 0.01$  and \*\*\* $P < 0.001$  compared with the control group. #### $P < 0.001$  compared with the s.c.-shIFIT2 group.

## Discussion

Many clinical conditions, such as food intake, chronic disease and treatment, can interfere with the classification of cancer cachexia and the identification of related inflammatory cytokines. Therefore, cancer cachexia is mainly studied in animal models, such as C26 and Mac16 mouse models.<sup>22,23</sup> However, the existing cachexia animal models have several limitations. In humans, the tumour burden is often  $<1\%$  when there is profound cachexia.<sup>5</sup> However, in many cachexia animal models, tumours reach  $>10\%$  of body mass, acting as a 'nitrogen trap'.<sup>24</sup> On the other hand, these cachexia animal models are allografts; it is difficult to clarify tumour-derived factors from the host response. In the present study, the smaller tumour size in i.v.-shIFIT2 mice (mean 0.67 g, approximately 1.9% of IBW) compared with s.c.-shIFIT2 mice (mean 1.3 g, approximately 3.8% of IBW) could underlie the cachectic phenotype, indicating that tumour burden is an independent factor in shIFIT2 depletion-induced cachexia. In addition, the shIFIT2 cachexia model is a xenograft mouse model; therefore, it is easier to differentiate tumour-derived and host-derived factors involved in cachexia pathogenesis. Thus, the shIFIT2 cachexia model may better mimic clinical cachexia and be a useful animal model for exploring the mechanisms of metastasis-related cachexia.

No significant changes in spleen and liver weight were observed in the cachectic i.v.-shIFIT2 mice. However, s.c.-shIFIT2

mice had higher spleen and liver weights than did healthy control mice. Histological examination revealed no metastasis or obvious pathogenic alterations in the livers and spleens of these four groups, suggesting that the higher liver and spleen weights in the s.c.-shIFIT2 group were not due to metastasis or pathogenic alterations. Splenomegaly commonly occurs in tumour cell transplantable models, including in C26 model.<sup>23</sup> Spleen weight has been identified to be positively correlated with tumour weight.<sup>25</sup> Of these four groups, mice in the s.c.-shIFIT2 group had the highest tumour weight; therefore, we suggest that the higher spleen weight in s.c.-shIFIT2 mice may be associated with the higher tumour weight, which may be positively correlated with the percentage of tumour-promoting immune cells, such as myeloid-derived suppressor cells (MDSCs).<sup>25</sup>

The liver plays a pivotal role in systemic inflammation, acute phase protein synthesis and gluconeogenesis, which have been documented in advanced cancer.<sup>26</sup> Compared with healthy control mice, s.c.-shCTRL mice showed no significant difference in serum CRP and albumin levels, indicating that systemic inflammation is not the major cause of liver weight gain. One mechanism that potentially contributed to the liver weight gain in s.c.-shIFIT2 mice is energy imbalance. The presence of a tumour may induce aberrant resting energy expenditure, in part due to futile substrate cycles, and thereby alter liver weight.<sup>27</sup> The energetic demands of a tumour, therefore, have the potential to substantially impact energy expenditure in tumour-bearing mice. Additional anal-

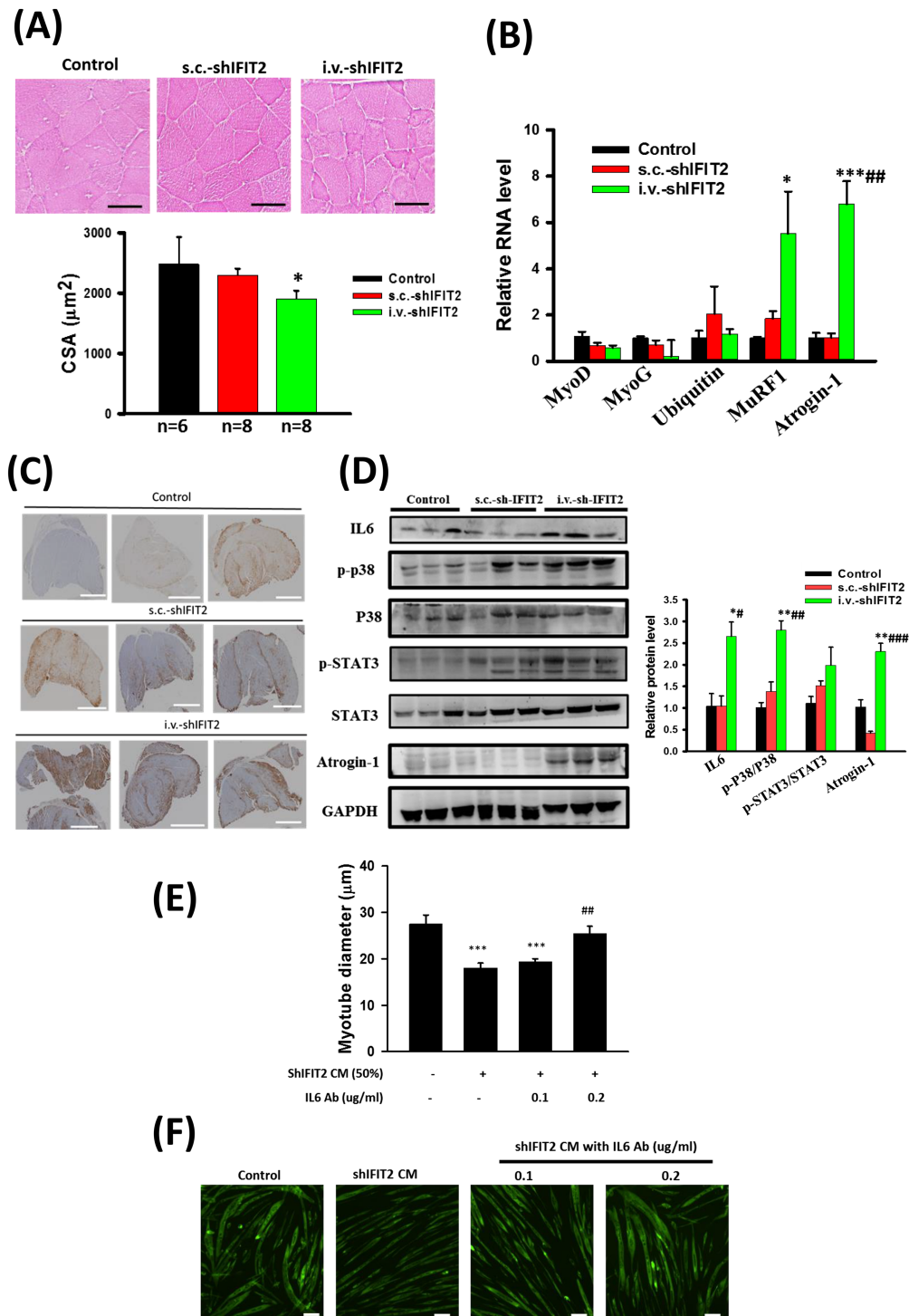


**Figure 5** Muscle atrophy is associated with IL6/p38 signalling in the shIFIT2 cachexia model. (A) Representative photomicrograph of haematoxylin and eosin-stained sections of gastrocnemius muscle and quantification of the cross-sectional area (CSA) from each group. Scale bar = 50  $\mu\text{m}$ . (B) The mRNA levels of MyoD, MyoG, ubiquitin, MuRF1 and atrogin-1 in gastrocnemius muscles from each group were examined by Q-PCR. Gene expression was normalized to GAPDH levels. (C) Immunohistochemistry of IL6 expression in control, s.c.-shIFIT2 and i.v.-shIFIT2 mice ( $n = 3$  per group). Scale bar = 2 mm. (D) The protein levels of IL6, phospho-p38, p38, phospho-STAT3, STAT3 and atrogin-1 in gastrocnemius muscle in each group were determined by western blotting ( $n = 3$  per group). GAPDH served as a loading control. (E) Diameter and (F) representative images of fluorescent myotubes from 72-h control, shIFIT2 conditioned medium (shIFIT2 CM) with or without IL6 Ab. Green indicates myosin 4 staining. Scale bar = 100  $\mu\text{m}$ . Data are presented as the mean  $\pm$  SEM. \* $P < 0.05$ , \*\* $P < 0.01$  and \*\*\* $P < 0.001$  compared with the control group. # $P < 0.05$ , ## $P < 0.01$  and ### $P < 0.001$  compared with the s.c.-shIFIT2 or the shIFIT2 CM group.

yses, such as those of hepatic triglycerides, inflammatory gene expression, energy metabolism and resting energy expenditure, will be needed to address the cause of increased liver weight in the s.c.-shIFIT2 model.

The present study used an experimental metastasis animal model that lacks a primary tumour to compare the i.v.-shIFIT2 and i.v.-shCTRL groups. It has been reported that the lungs are the primary location of experimental metastasis in animal models, as we found in the i.v.-shCTRL group. Interestingly, we found that i.v.-shCTRL mice had multiple metastatic nodules in the lungs but did not develop cachexia symptoms. However, IFIT2-depleted cells effectively extravasated from vascular and lymphatic vessels, thereby enhancing the metastatic tropism of OSCC cells to multiple sites in mice.<sup>14</sup> Moreover, we found that cachexia syndrome is not related to specific metastasis sites (Table 1), indicating that cachexia induced by IFIT2-depleted metastatic tumours is not induced by the presence of metastasis at specific sites. These results indicate that IFIT2 depletion may be a trigger during metastasis-induced cachexia.

In the shIFIT2 cachexia model, several tumour-derived and host-derived cytokines were identified, including GM-CSF, GRO $\alpha$ , IL6, IL8, IL18, IP10, CCL2, CCL22, TNF $\alpha$  and G-CSF. The levels of TNF $\alpha$ , IL6, IL8, IP10 and CCL2 are elevated in cachectic cancer patients.<sup>6,28,29</sup> In addition, increased circulating CRP levels and decreased albumin levels, which serve as cancer cachexia biomarkers,<sup>30</sup> were observed in cachectic i.v.-shIFIT2 mice. These results suggest the strong association of inflammation and the cachexia phenotype in the shIFIT2 cachexia model. Leukaemia inhibitory factor (LIF), an IL6 family cytokine, is a cachectic factor in various animal cachexia models.<sup>19,31,32</sup> LIF has been linked to cachexia-associated muscle wasting, lipolysis, IL6 and G-CSF increase.<sup>19,32,33</sup> In the present study, we found that no significant difference in host-derived LIF level between these four groups (Table 3). However, we did not examine the tumour-derived LIF level between these four groups. Whether tumour-derived LIF is required for the production of IL6 and G-CSF, muscle wasting, lipolysis in the shIFIT2 cachexia model will be further studied.

IL6 is a key link between chronic inflammation and tumour progression. IL6 is produced in the tumour by tumour-infiltrating immune cells, stromal cells and the tumour cells themselves.<sup>34</sup> IL6 also induces the production of proinflammatory and angiogenesis-promoting factors, such as IL8, CCL2, GM-CSF and VEGF, which act in an autocrine and/or paracrine fashion on immune and non-immune cells within the tumour microenvironment.<sup>35</sup> A previous study detected significantly higher level of IL6 in HNC patients than in controls.<sup>36</sup> IL6 has been found to play roles in EMT in HNC cell lines thereby promoting regional and distant metastasis.<sup>37</sup> In the present study, we demonstrate that the IL6/p38/Atrogin-1 axis may be associated with muscle atrophy in the cachectic shIFIT2 mice. Future studies inhibiting IL6 signalling by means

of monoclonal Ab or genetic approaches will be needed to explore the involvement of IL6 on inflammation, metastasis and cachexia in the shIFIT2 cachexia model.

The limitation of this study is the lack of a thorough mechanism linking IFIT2 to cachexia. Our past studies demonstrated that IFIT2 depletion through genetic silencing in non-metastatic CAL27 cells results in metastasis linked to EMT, TNF $\alpha$  overexpression and in vivo angiogenesis.<sup>14,16</sup> Clinically, OSCC patients expressing low levels of IFIT2 have a poor prognosis than those expressing high levels<sup>13</sup>; the median postsurgery survival for stage IV patients with high IFIT2 expression was reported to be 66.5 months, whereas that for patients with low IFIT2 expression was 13.6 months ( $P < 0.01$ ). A negative relationship between IFIT2 expression and distant metastasis rate was observed in a clinical study.<sup>14</sup> In the present study, we further demonstrate that inflammation may be the key cause of cachexia in i.v.-shIFIT2 mice. IFIT2 may play a key role in regulating the inflammatory tumour environment during metastasis, which leads to cachexia. IFIT2 is a critical signalling intermediate for lipopolysaccharide (LPS)-induced inflammation, including the secretion of TNF $\alpha$  and IL6.<sup>38</sup> IFIT2 overexpression represses LPS induced TNF $\alpha$  expression at posttranscriptional levels.<sup>39</sup> However, the in vivo function of IFIT2 in the inflammatory response during cancer metastasis and cachexia is still unknown, indicating the need for more studies. In addition to IFIT2 silencing in nonmetastatic OSCC cells, additional strategies such as IFIT2 overexpression in metastatic OSCC cells, such as UMSCC2<sup>40</sup> should be applied to clarify the involvement of IFIT2 in metastasis and cachexia.

Cachexia could be considered a hallmark of metastatic cancer because these two conditions are well correlated in the clinic. However, few studies have used animal models to define the involvement of metastasis in cachexia. Our model will aid in identifying molecular mediators that could be effectively targeted to improve cachexia associated with metastasis.

## Acknowledgements

The authors certify that they comply with the ethical guidelines for authorship and publishing in the *Journal of Cachexia, Sarcopenia and Muscle*.<sup>41</sup> This study was supported by grants from the Ministry of Science and Technology, Taiwan (MOST 108-2320-B-320-004, MOST 109-2320-B-182-044 and MOST 110-2320-B-182-023 MY3) and Chang Gung Memorial Hospital, Taoyuan City, Taiwan (CMRPD1L0201) to Kuo-Chu Lai and from Hualien Tzu Chi Hospital, Taiwan (TCRD108-65) to Jyh-Gang Hsieh. We thank the Taiwan Mouse Clinic, Academia Sinica and Taiwan Animal Consortium for technical support in whole-body composition assessments and food and water intake measurements.

## Online supplementary material

Additional supporting information may be found online in the Supporting Information section at the end of the article.

## Conflict of interest

The authors declare no conflict of interest.

## References

1. Fearon K, Strasser F, Anker SD, Bosaeus I, Bruera E, Fainsinger RL, et al. Definition and classification of cancer cachexia: an international consensus. *Lancet Oncol* 2011; **12**:489–495.
2. von Haehling S, Anker SD. Cachexia as a major underestimated and unmet medical need: facts and numbers. *J Cachexia Sarcopenia Muscle* 2010; **1**:1–5.
3. Tan BH, Fearon KC. Cachexia: prevalence and impact in medicine. *Curr Opin Clin Nutr Metab Care* 2008; **11**:400–407.
4. Mondello P, Mian M, Aloisi C, Fama F, Mondello S, Pitini V. Cancer cachexia syndrome: pathogenesis, diagnosis, and new therapeutic options. *Nutr Cancer* 2015; **67**:12–26.
5. Fearon KC, Glass DJ, Guttridge DC. Cancer cachexia: mediators, signaling, and metabolic pathways. *Cell Metab* 2012; **16**:153–166.
6. Inacio Pinto N, Carnier J, Oyama LM, Otoch JP, Alcantara PS, Tokeshi F, et al. Cancer as a proinflammatory environment: metastasis and cachexia. *Mediators Inflamm* 2015; **2015**:791060. <https://doi.org/10.1155/2015/791060>
7. Chen JL, Walton KL, Qian H, Colgan TD, Hagg A, Watt MJ, et al. Differential effects of IL6 and activin A in the development of cancer-associated cachexia. *Cancer Res* 2016; **76**:5372–5382.
8. Bonetto A, Aydogdu T, Kunzevitzky N, Guttridge DC, Khuri S, Koniaris LG, et al. STAT3 activation in skeletal muscle links muscle wasting and the acute phase response in cancer cachexia. *PLoS One* 2011; **6**:e22538. <https://doi.org/10.1371/journal.pone.0022538>
9. Ulker N, Samuel CE. Mechanism of interferon action. II. Induction and decay kinetics of the antiviral state and protein P54 in human amnion U cells treated with gamma interferon. *J Biol Chem* 1987; **262**:16804–16807.
10. Reich NC. A death-promoting role for ISG54/IFIT2. *J Interferon Cytokine Res* 2013; **33**:199–205.
11. Su W, Xiao W, Chen L, Zhou Q, Zheng X, Ju J, et al. Decreased IFIT2 expression in human non-small-cell lung cancer tissues is associated with cancer progression and poor survival of the patients. *Onco Targets Ther* 2019; **12**:8139–8149.
12. Chen L, Zhai W, Zheng X, Xie Q, Zhou Q, Tao M, et al. Decreased IFIT2 expression promotes gastric cancer progression and predicts poor prognosis of the patients. *Cell Physiol Biochem* 2018; **45**:15–25.
13. Lai KC, Chang KW, Liu CJ, Kao SY, Lee TC. IFN-induced protein with tetratricopeptide repeats 2 inhibits migration activity and increases survival of oral squamous cell carcinoma. *Mol Cancer Res* 2008; **6**:1431–1439.
14. Lai KC, Liu CJ, Chang KW, Lee TC. Depleting IFIT2 mediates atypical PKC signaling to enhance the migration and metastatic activity of oral squamous cell carcinoma cells. *Oncogene* 2013; **32**:3686–3697.
15. Regmi P, Lai KC, Liu CJ, Lee TC. SAHA overcomes 5-FU resistance in IFIT2-depleted oral squamous cell carcinoma cells. *Cancers (Basel)* 2020; **12**:3527.
16. Lai KC, Liu CJ, Lin TJ, Mar AC, Wang HH, Chen CW, et al. Blocking TNF- $\alpha$  inhibits angiogenesis and growth of IFIT2-depleted metastatic oral squamous cell carcinoma cells. *Cancer Lett* 2016; **370**:207–215.
17. Ku WT, Tung JJ, Lee TJ, Lai KC. Long-term exposure to oroxylin A inhibits metastasis by suppressing CCL2 in oral squamous cell carcinoma cells. *Cancers (Basel)* 2019; **11**:353.
18. Bonetto A, Andersson DC, Waning DL. Assessment of muscle mass and strength in mice. *Bonekey Rep* 2015; **4**:732.
19. Kandarian SC, Nosacka RL, Delitto AE, Judge AR, Judge SM, Ganey JD, et al. Tumour-derived leukaemia inhibitory factor is a major driver of cancer cachexia and morbidity in C26 tumour-bearing mice. *J Cachexia Sarcopenia Muscle* 2018; **9**:1109–1120.
20. Betancourt A, Busquets S, Ponce M, Toledo M, Guardia-Olmos J, Pero-Cebollero M, et al. The animal cachexia score (ACASCO). *Animal Model Exp Med* 2019; **2**:201–209.
21. Deboer MD. Animal models of anorexia and cachexia. *Expert Opin Drug Discov* 2009; **4**:1145–1155.
22. Bing C, Brown M, King P, Collins P, Tisdale MJ, Williams G. Increased gene expression of brown fat uncoupling protein (UCP)1 and skeletal muscle UCP2 and UCP3 in MAC16-induced cancer cachexia. *Cancer Res* 2000; **60**:2405–2410.
23. Bonetto A, Rupert JE, Barreto R, Zimmers TA. The colon-26 carcinoma tumor-bearing mouse as a model for the study of cancer cachexia. *J Vis Exp* 2016; **30**:54893.
24. Carrascosa JM, Martinez P, Nunez de Castro I. Nitrogen movement between host and tumor in mice inoculated with Ehrlich ascitic tumor cells. *Cancer Res* 1984; **44**:3831–3835.
25. Jiang W, Li Y, Zhang S, Kong G, Li Z. Association between cellular immune response and spleen weight in mice with hepatocellular carcinoma. *Oncol Lett* 2021; **22**:625.
26. Liefvers JR, Mourtzakis M, Hall KD, McCargar LJ, Prado CM, Baracos VE. A viscerally driven cachexia syndrome in patients with advanced colorectal cancer: contributions of organ and tumor mass to whole-body energy demands. *Am J Clin Nutr* 2009; **89**:1173–1179.
27. Purcell SA, Elliott SA, Baracos VE, Chu QS, Prado CM. Key determinants of energy expenditure in cancer and implications for clinical practice. *Eur J Clin Nutr* 2016; **70**:1230–1238.
28. Talbert EE, Lewis HL, Farren MR, Ramsey ML, Chakedis JM, Rajasekera P, et al. Circulating monocyte chemoattractant protein-1 (MCP-1) is associated with cachexia in treatment-naïve pancreatic cancer patients. *J Cachexia Sarcopenia Muscle* 2018; **9**:358–368.
29. Lerner L, Tao J, Liu Q, Nicoletti R, Feng B, Krieger B, et al. MAP3K11/GDF15 axis is a critical driver of cancer cachexia. *J Cachexia Sarcopenia Muscle* 2016; **7**:467–482.
30. Cao Z, Zhao K, Jose I, Hoogenraad NJ, Osellame LD. Biomarkers for cancer cachexia: a mini review. *Int J Mol Sci* 2021; **22**. <https://doi.org/10.3390/ijms22094501>
31. Mori M, Yamaguchi K, Honda S, Nagasaki K, Ueda M, Abe O, et al. Cancer cachexia syndrome developed in nude mice bearing melanoma cells producing leukemia-inhibitory factor. *Cancer Res* 1991; **51**:6656–6659.
32. Seto DN, Kandarian SC, Jackman RW. A key role for leukemia inhibitory factor in C26 cancer cachexia. *J Biol Chem* 2015; **290**:19976–19986.
33. Arora GK, Gupta A, Narayanan S, Guo T, Iyengar P, Infante RE. Cachexia-associated adipose loss induced by tumor-secreted leukemia inhibitory factor is counterbalanced by decreased leptin. *JCI Insight* 2018; **3**. <https://doi.org/10.1172/jci.insight.121221>
34. Johnson DE, O'Keefe RA, Grandis JR. Targeting the IL-6/JAK/STAT3 signalling axis in cancer. *Nat Rev Clin Oncol* 2018; **15**:234–248.
35. Mullberg J, Geib T, Jostock T, Hoischen SH, Vollmer P, Voltz N, et al. IL-6 receptor independent stimulation of human gp130 by viral IL-6. *J Immunol* 2000; **164**:4672–4677.
36. Bussu F, Graziani C, Gallus R, Cittadini A, Galli J, E DEC, et al. IFN-gamma and other serum cytokines in head and neck squamous cell carcinomas. *Acta Otorhinolaryngol Ital* 2018; **38**:94–102.

37. Yadav A, Kumar B, Datta J, Teknos TN, Kumar P. IL-6 promotes head and neck tumor metastasis by inducing epithelial-mesenchymal transition via the JAK-STAT3-SNAIL signaling pathway. *Mol Cancer Res* 2011;**9**:1658–1667.
38. Siegfried A, Berchtold S, Manncke B, Deuschle E, Reber J, Ott T, et al. IFIT2 is an effector protein of type I IFN-mediated amplification of lipopolysaccharide (LPS)-induced TNF-alpha secretion and LPS-induced endotoxin shock. *J Immunol* 2013; **191**:3913–3921.
39. Berchtold S, Manncke B, Klenk J, Geisel J, Autenrieth IB, Bohn E. Forced IFIT-2 expression represses LPS induced TNF-alpha expression at posttranscriptional levels. *BMC Immunol* 2008;**9**:75.
40. Bais MV, Kukuruzinska M, Trackman PC. Orthotopic non-metastatic and metastatic oral cancer mouse models. *Oral Oncol* 2015;**51**:476–482.
41. von Haehling S, Morley JE, Coats AJS, Anker SD. Ethical guidelines for publishing in the Journal of Cachexia, Sarcopenia and Muscle: update 2021. *J Cachexia Sarcopenia Muscle* 2021;**12**:2259–2261.